JOURNAL OF ADVANCED MECHANICAL ENGINEERING APPLICATIONS
e-ISSN: 2716-6201

JAMEA

Vol. 5 No. 1 (2024) 36-45
https://publisher.uthm.edu.my/ojs/index.php/jamea

Numerical Study of Vortex Effect on Splitter Plate under Turbulence Flow over Circular Cylinder

Mathan Sambu[1,3*], Izzuddin Zaman[1], Bukhari Manshoor[1], Nagentrau Muniandy[2], Vin Cent Tai[3]

[1] *Faculty of Mechanical and Manufacturing Engineering, Universiti Tun Hussein Onn Malaysia, Parit Raja, Batu Pahat, Johor, MALAYSIA*
[2] *School of Engineering, Faculty of Innovation & Technology, Taylor's University, Subang Jaya, Selangor, MALAYSIA*
[3] *Faculty of Engineering, Built Environment and Information Technology, SEGi Universiti, Petaling Jaya, Selangor, MALAYSIA*

*Corresponding Author: gd200040@student.uthm.edu.my
DOI: https://doi.org/10.30880/jamea.2024.05.01.006

Article Info

Received: 6 November 2023
Accepted: 12 February 2024
Available online: 30 June 2024

Keywords

Vortex shedding, turbulence flow, reynolds number, strouhal number, ANSYS fluent, vorticity

Abstract

Vortex shedding is commonly observed in both natural and artificial situations. Two key variables, the blockage ratio and the Reynolds number, determine the flow characteristics around a confined bluff body. The goal of the current study was to apply numerical simulation to examine the development of vortices in a continuous turbulence flow at the distanced position of a single splitter plate. As a starting point, the flow around a fixed circular cylinder and plate is examined at various spaced position ratios, where *L ratios are defined as the distance between the cylinder's centre and the plate's front edge. In the wake of the cylinder, when *L is raised, positive and negative vortices are generated. The pressure distribution following the vortex shedding core strike is felt at the plate face tip (starting edge). Compared to the other two positions, the CL created by L2 is larger and receives better cortex hits.

1. Introduction

The study of flow around a bluff body has long been considered a fundamental challenge, given its prevalence in natural phenomena and widespread use in engineering applications. A typical scenario involves a bluff body positioned within a symmetrical two-dimensional channel (2D), whose motion is constrained by stationary no-slip walls under a finite volume technique. The resulting confinement significantly alters the flow's behaviour, potentially leading to changes in hydrodynamic forces, heat transfer, and mass transfer properties of the body [1, 2]

Vortex flowmeters, which may be utilised regardless of the fluid phase, are one of these industrial use areas for flow measurement. The measurement of vortex shedding frequency, also known as von Karman Vortex Street in the wake zone of bluff bodies, is the core working principle of these fundamentals. The Strouhal number does not vary as the vortex shedding frequency and free stream velocity change correspondingly, like the von Karman Vortex Street [3]. Vortex streets are commonly observed in various natural and man-made environments. For instance, they can be spotted in river currents downstream of bridge support columns and in the wake of steady winds blowing past the bridges, smokestacks, transmission lines, and missiles preparing to launch vertically. In addition, above-ground pipelines in arid regions of the world can also generate vortex streets [4, 5].

Nomenclature:	
β	blockage ratio
D	height of the bluff body
H	height of the channel
ρ	fluid density
U_∞	freestream velocity
μ	dynamic viscosity
Re	Reynolds numbers
C_L	lift coefficients
C_D	drag coefficients
f	frequency of vortex shedding
St	Strouhal number
ν	kinematic viscosity
L	characteristic length

The flow characteristics around a confined bluff body are determined by two fundamental parameters, as reported in the literature: the blockage ratio (β = D/H), where D represents the height of the bluff body and H belongs to height of the channel, and the Reynolds number ($Re = \rho U_\infty D / \mu$), where ρ denotes the fluid density, U_∞ is the free-stream velocity, and μ is the dynamic viscosity of the fluid.

Confined flow displays distinct characteristics from unconfined scenarios, particularly regarding vortex shedding patterns. An intriguing phenomenon is the complete suppression of alternating vortex shedding when the cylinder is close to the confinement wall (or when β is sufficiently large), as first noted by Shair et al. in 1963 [6]. This article briefly reviews published research on the confined flow around three typical bluff body shapes: circular cylinder, square cylinder, and flat plate. The focus is on the effects of β and Re on each shape's flow structure.

Fluid flow behaviour around various bluff body shapes has been the subject of extensive research into the flow behind bluff bodies for many years [7-11]. In the experiment conducted by researcher Islam (2017), the laminar flow behind a square cylinder was examined using low Reynolds numbers (Re = 100 and 160). This study describes and explores the crucial flow physics of various observed flow patterns in terms of instantaneous vorticity contour visualisation, time-trace analysis of drag and lift coefficients (C_D, C_L), and power spectra analysis of force coefficient [12].

Another research by Kumar studied the flow behind a square-shaped bluff body situated in a confined finite region domain. Under the Reynolds number Re=100, the constant velocity flow has been studied. Streamline pattern, vorticity contours, lift-drag coefficients, and their accompanying power spectra are used to display the results. It has been shown that both Re and K have a significant influence on the vortex-shedding phenomena [13]. In the research conducted by author Dey, a two-dimensional steady laminar flow has been numerically examined at low Reynolds numbers between 5 and 45, under various corner radius conditions, and utilising a blockage value of 0.05. Under this Re, it is discovered that the boundary layer thickness and the displacement thickness decrease as the corner radius is reduced. Decreasing Re also causes the boundary layer profile to shift downward [14].

The study of circular cylinder shapes as bluff bodies has been the subject of an expanding body of literature in recent years [15-19]. In an earlier experiment, flow characteristics around a modified circular cylinder were examined at a Reynolds number of $Re = 2.67\times10^4$. The experiment investigated changing a circular cylinder with a slit perpendicular to the incoming airflow to establish a channel for flow communication between the windward and leeward stagnation regions. According to the findings of the experiments, a slit contributes to lessening the drag force and decreasing the amplitude fluctuations of the dynamic wind loads operating on the test model. Additionally, a flip-flop phenomenon is observed, and the frequency of dimensionless vortices is seen to be switched to a deficient level [20].

Previous studies have used experiments to study the cross-flow around a circular cylinder positioned close to the wall of a channel with a rectangular cross-section. Utilising flow visualisation and SIV measurements of instantaneous velocity fields, the researcher investigated the flow pattern evolution behind the cylinder and the formation of regular vortex structures. The visualisation concludes that the shear layer instability causes the laminar to have a turbulent transition in the cylinder's wake [21].

In recent research, numerical analysis by Sharma and team examined incompressible and unsteady flow via a slotted circular cylinder in the laminar regime. The simulation computes the flow field in the 60–180 Reynolds number range, classified as laminar. According to the results, all Re ranges had periodic vortex shedding, and the slotted cylinders successfully suppressed it. For Re more than 70, the slotted cylinders' overall drag coefficient was lower than that of the unslotted cylinders [22]. In a previous computational study, the flow and heat transfer structure was examined around a very slim bluff body with a rectangular cross-sectional area. The conditional

Reynolds number is 100; it is assumed that the flow is laminar for this investigation because it is so low. According to the simulations, the stagnation point is moved from the centre to a position on the frontal side by changing the bluff body's incidence angle. More than 95% of net drag and a third of lift forces are attributed to the pressure component, according to the bluff body's under 45-degree angle of incidence [23].

In summary, it has been demonstrated from this review that there have been few studies exploring vortex-shedding flow in turbulent conditions. Based on that, the goal of the current work was to use numerical simulation to investigate the generation of vortices under continuous turbulence flow in varied with the distanced positions of the single splitter plate.

2. Theoretical Background

The concept of flow instability can explain the theoretical basis of vortex shedding. A zone of low pressure develops behind a bluff body when a fluid flowing around it separates at some point. The regions of fluid revolving around a central axis can emerge because of this low-pressure area, creating vorticities. The formation of these vortices depends on the flow Reynolds number, which is a dimensionless quantity that describes the ratio of inertial forces to viscous forces in the fluid. The flow becomes unstable, and vortices form as the Reynolds number rises above a particular point. The nonlinear interaction between the fluid flow and the vortices themselves, which can intensify and perpetuate the vortex-shedding process, is the cause of this instability [24]. Another dimensionless number that expresses the correlation between the shedding frequency and fluid velocity is the Strouhal number, also called the shedding frequency.

2.1 Strouhal Background

The frequency of vortex shedding is related to the fluid velocity and the size and shape of a body in a fluid flow by a dimensionless quantity known as the Strouhal number (St). It is defined as the ratio of vortex shedding frequency to the sum of the fluid velocity and the body's characteristic dimension. The Strouhal number is given by:

$$\mathrm{St} = \frac{f.\mathrm{D}}{\mathrm{U}_\infty} \tag{1}$$

Where St is the Strouhal number, f is the frequency of vortex shedding, D is the characteristic dimension of the bluff body, and U_∞ is the freestream fluid velocity. The Strouhal number is an essential parameter in fluid dynamics, as it provides a means of characterising and predicting vortex-shedding behaviour for different geometries and flow conditions [25].

2.2 Reynolds Number

The ratio of inertial to viscous forces in a fluid is the Reynolds number (Re). The Reynolds number is given by:

$$\mathrm{Re} = \frac{\mathrm{UL}}{v} \tag{2}$$

Where U is the fluid's velocity, L is the flow's characteristic length scale, and v is the kinematic viscosity of the fluid. The Reynolds number controls fluid flow, with laminar flow occurring at low Reynolds numbers and turbulent flow occurring at high Reynolds numbers. Understanding the Reynolds number is essential in various disciplines, including fluid mechanics, aerodynamics, and heat transport [26].

3. Numerical Modelling

The simulation is conducted under constant air flow velocity, corresponding to Re = 104. To simulate, a 2D model schematic of the CFD domain with a circular cylinder plate where the plate was positioned at varied distances in the wake of the cylinder is shown in Fig. 1.

Fig. 1 shows three different distanced positions *L from the cylinder as samples of the mounted plate. The numerical models employed under 50D × 20D as computational domain. The circular cylinder positions 10D and 40D, respectively, to reduce the impact of inlet and outlet effects. This simulation aims to investigate and obtain the coefficient of drag and lift behaviour of the plate, which is under varied positions. The development of vorticity behind the circular cylinder to identify the vortex shedding together identifies pressure distribution around the bluff body and plate since this study investigates the plate's behaviour under three different positions required to create individual domains with dimensions for the simulation, as listed in Table 1.

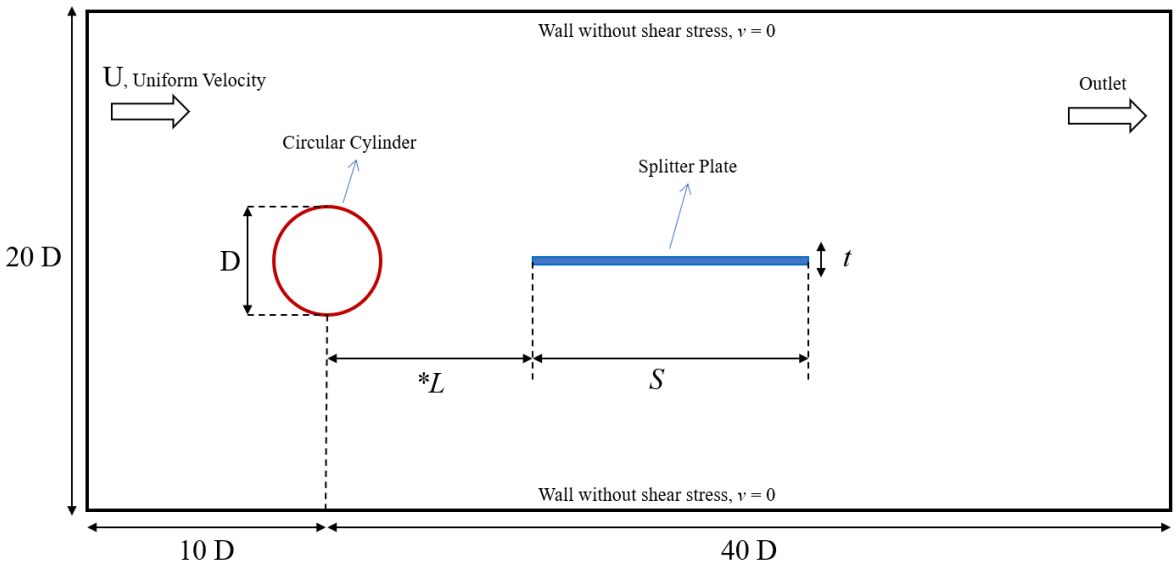

Fig. 1 *Schematic of the computational domains flow around circular cylinder and plate, including boundary conditions*

Table 1 *Physical properties values of the domain geometry structures*

Bluff Bodies	Properties / Dimensions	Symbol	Value (unit) / Description
Circular Cylinder	Diameter	D	0.01 (m)
	Surface	Smt.	Smooth
Splitter Plate	Thickness	t	0.0004 (m)
	Span	S	0.04 (m)
	Distance, *L	L_1	4D
		L_2	5D
		L_3	6D

3.1 Validation of Mesh Independency

The entire domain was split into several faces using a structured block method to create better meshing. The surface body's meshing is set to a quadrilateral mesh with a maximum element size of 0.026 m to generate a fine and even mesh throughout. At the same time, the sizing of each edge is divided by a selected number of division methods. By developing this, the meshing will be dispersed equally throughout the bluff body and domain by its shape, where the mesh skewness maximum achieved around 0.5. Fig. 2 visualises the domain's mesh outcome and structured mesh around the bluff bodies

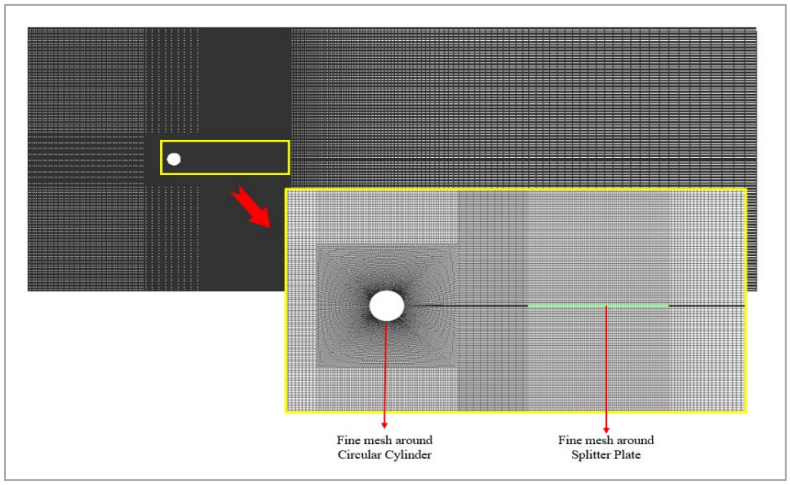

Fig. 2 *Mesh grid distribution of the boundary (fluid) domain*

J. of Advanced Mechanical Engineering Applications Vol. 5 No. 1 (2024) p. 36-45

Several mesh independency experiments for flow around the cylinder were conducted as initiating benchmarks for the investigation. A set of grid-independent experiments with three structured mesh models of different mesh element counts were performed on a single circular cylinder under Re 100. An overview of the variations in the drag and lift coefficients concerning the number of grids is shown in Table 2.

Table 2 *Mesh independency examinations of a single circular cylinder at Re = 100*

Flow Characteristics	**Number of grid elements**			
	Type 1 ≈40,000	Type 2 ≈58,000	Type 3 ≈76,000	Type 4 ≈98,000
Drag Coefficient, C_D	1.315	1.326	1.337	1.338
Drag Coefficient, C_L	0.216	0.224	0.235	0.237

Table 3 compares the published results at laminar flows and a single circular cylinder's drag and lift coefficients at a comparable Re. It has been noted that there is good agreement between the time-averaged values of the fluctuating lift coefficient (C_L) and the drag coefficient (C_D) where researchers released the data. The comparison proved that Type 3 mesh elements can be used for the remaining simulations with reasonable accuracy.

Table 3 *Mesh independency examinations of a single circular cylinder at Re = 100*

References	C_D	C_L
Park, Kwon, & Choi [27]	1.33	0.235
Weilin Chen Chunning Ji (2020) [28]	1.336	0.230
Present – Mesh Type 3	1.337	0.235

3.2 Simulation Method

For this present CFD simulation, ANSYS FLUENT was used as computational software. Since the Re remains for all three domains (plate position), the FLUENT was set up into the turbulence-based model for all the analysis systems. The simulation initiates setting with a pressure-based type solver chosen with transient time setup and absolute velocity formulation in a planar coordinate system 2D space. According to Re, the boundary conditions of the inlet are uniform flow velocity launch. The cylinder surface, together with the top and bottom walls of the domain, has no-slip wall condition, and the outlet boundary was continually in zero pressure condition. Using air as flow fluid for this simulation, the properties where air density and dynamic viscosity are 1.225 kg/m^3 and 1.802x10^{-5} kg/m.s, respectively. The coupled scheme method under second-order implicit formulation is used to obtain precise results. The residual of convergence criteria has been reduced to generate more accurate results. The entire simulation per domain setup runs up to 1500 time steps under 0.00015-sec step size. Each time step required a maximum of 80 steps to iterate and meet the converge condition. Simulation initiates with Hybrid initialization and monitors the lift and drag coefficient of cylinder-plate bodies.

4. Result and Discussions

This section discusses the fluidic parameters in the model's boundary domain, including pressure, force coefficients, and vorticity after the bluff body.

4.1 Pressure Coefficient

The instantaneous pressure coefficient (C_P) is shown in Fig. 3 for distanced increments *L as L_1, L_2 and L_3. The pressure wake varies over time along the simulation. A similar time frame was selected to indicate these pressure coefficients, where the initial vortex shedding for every domain was used to make the comparison.

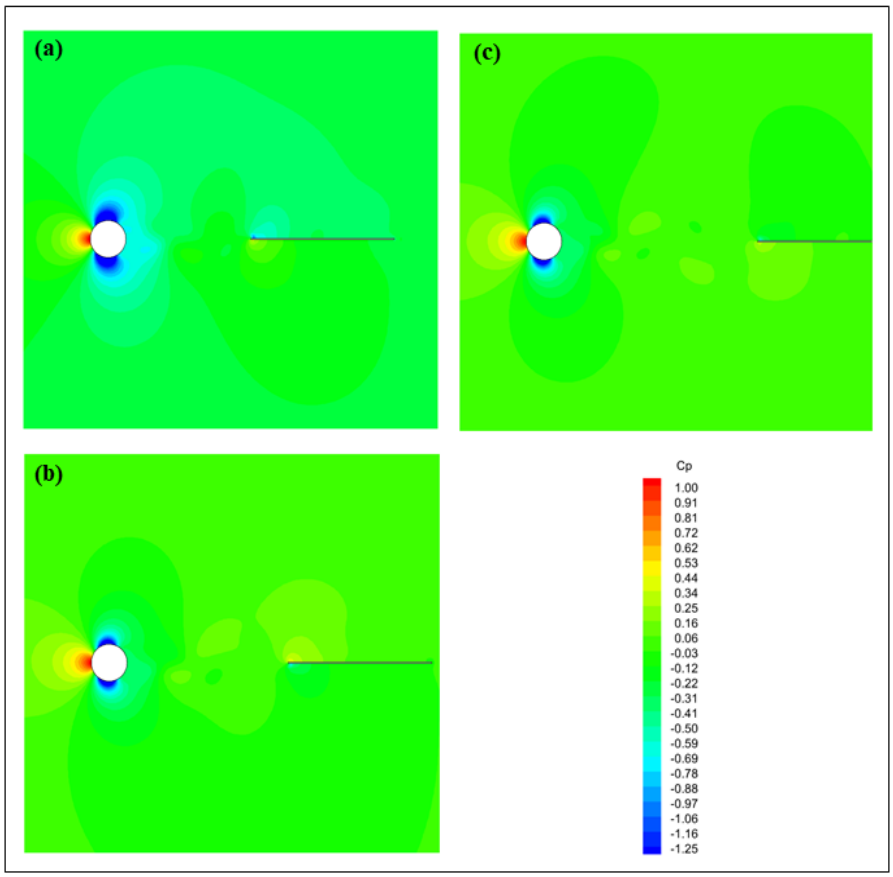

Fig. 3 *Pressure coefficient (C_P) distribution around the circular cylinder and plate different distance positioned; (a) L; (b) L_2 and (c) L_3*

As observed, the plate behind the bluff body is also subjected to differential pressure on each surface side, top and bottom. Fig. 3.a illustrates the development of the pressure in the cylinder's wake and the impact of the plate behind it in different range placements. The plate face tip (begin edge) experiences the pressure distribution after the vortex shedding core hit. This provides initial values of the pressure experienced by the plate. Moreover, both surfaces of the plate (top and bottom) begin to get the pressure coefficient consecutively once the vortex shedding develops fully and constantly.

4.2 Lift Coefficient

To better understand the expansion of forces, the lift coefficients and C_L of the cylinder (black plots in Fig. 4) and plate (blue plots in Fig. 4) are shown in Fig. 4 as a function of *L. All the C_L were plotted according to the selected period step as the initial stage of vortex development. It should be noted that the lift coefficients of the plate were computed based on the upstream circular cylinder diameter to give a meaningful comparison between the results. Observing Fig. 4, it is apparent that the cylinder creates a lesser amount of C_L compared to the plate, which almost reaches 0.8. Also, it is clearly visible that the L_2 position makes a large C_L compared to the other two positions, L_1 and L_3. A comparison of both cylinder and plate indicates that L_2 receives a better core vortex after the bluff body. Furthermore, it is understood that a slight spacing ratio difference can generate a fluctuated force experience for the plate. This also substantiates that the pressure coefficient for position L_2 getting more significant force was visible in Fig. 3 (b).

J. of Advanced Mechanical Engineering Applications Vol. 5 No. 1 (2024) p. 36-45

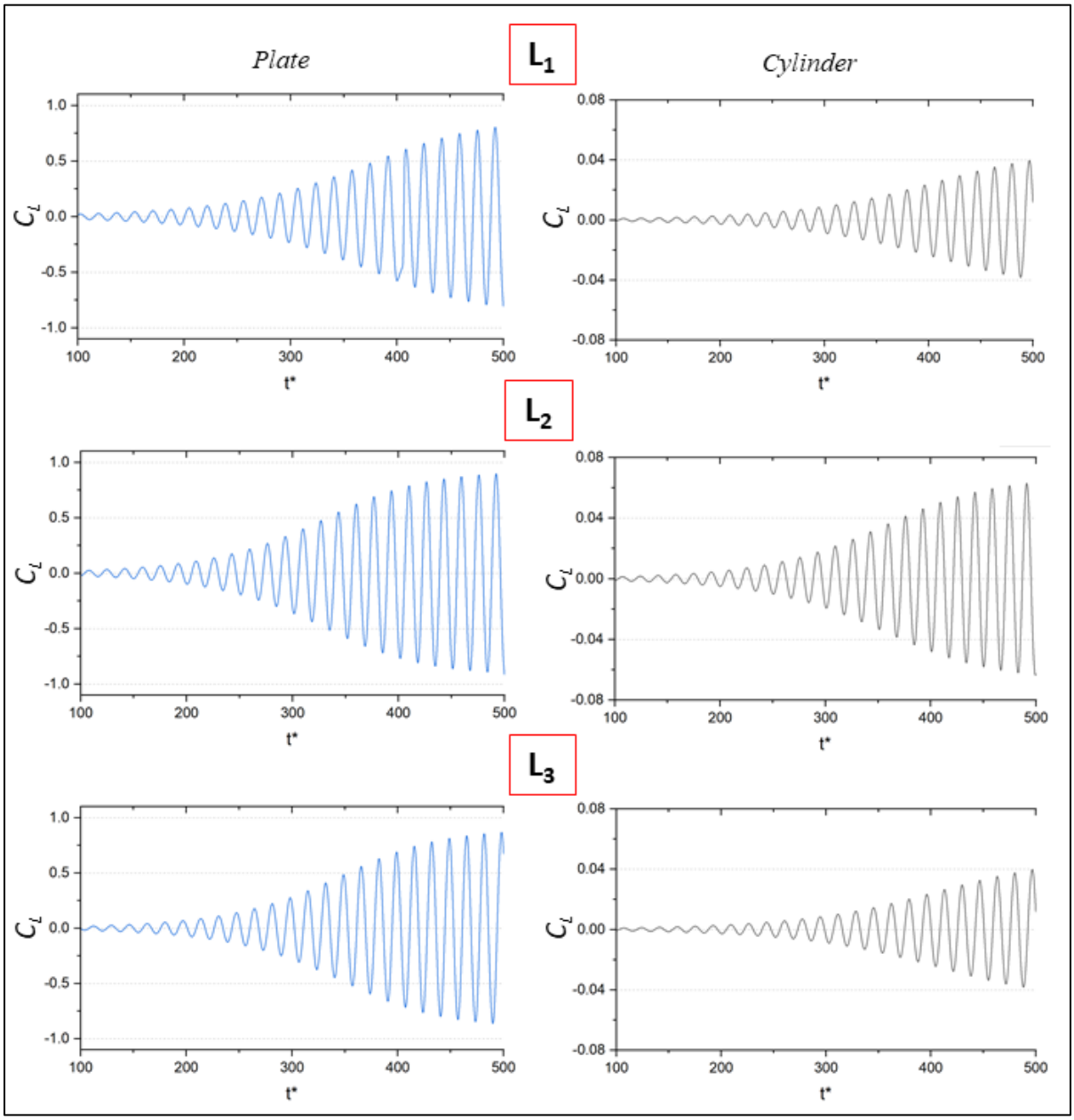

Fig. 4 *Lift coefficient (C_L) wake around the circular cylinder and plate different distance positioned; (a) L_1; (b) L_2; and (c) L_3*

4.3 Vorticity Comparison

At first, the flow around a fixed circular cylinder and plate is investigated at various spacing ratios, defined as the distance between the cylinder's centre and the plate's front edge. The position ratio varied from three difference spacing **L* with an increment similar to cylinder diameter, D. Fig. 5 shows the vorticity contours around the cylinder and plate at Re equivalent to 104. It has been discovered that when the spacing ratio between the cylinder and the plate is adjusted to the smallest tested value of L1 = 0.04m, generated shear layers from the upstream cylinder move downward with minimal to the plate. A similar pattern is also seen once distance increases as L2 and L3. In contrast, positive and negative vortices are formed in the wake of the cylinder when **L* is increased to 5D, and they freely migrate and attach to the downstream of the plate more vigorously. It also turns out that increasing the position ratio to 5D and 6D produces the most vorticity. Maximum vertical force is the lift that can be imparted to the plate to produce maximum deformation.

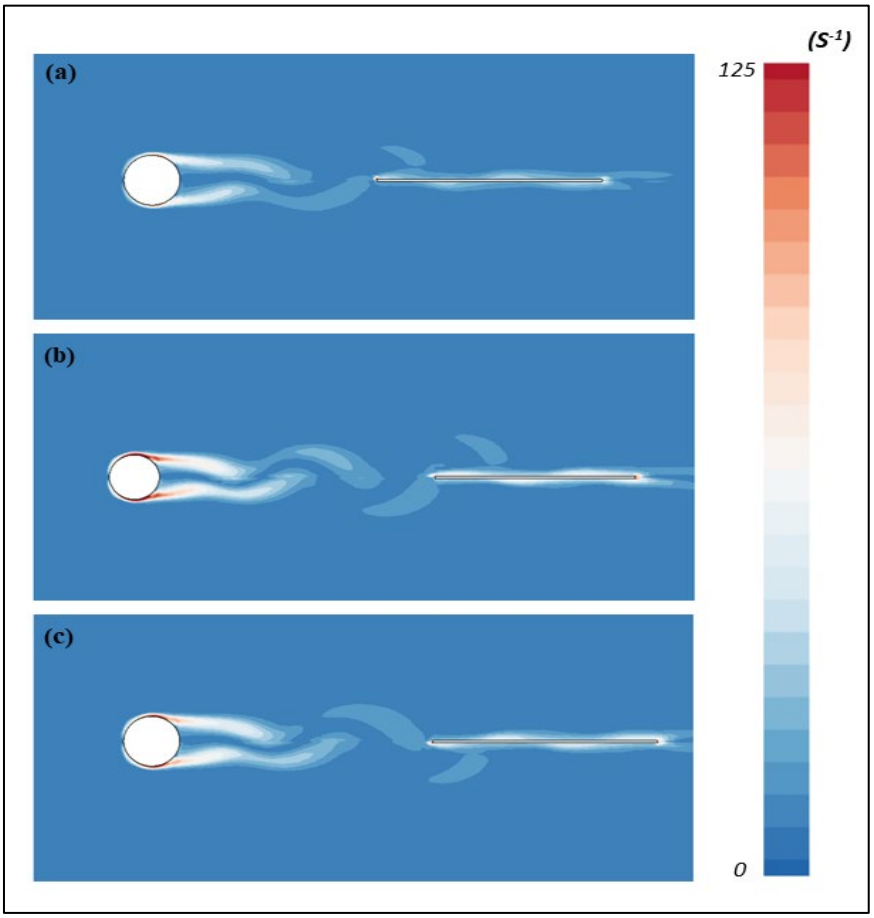

Fig. 6 *Vorticity contours around the stationary circular cylinder and plate at Re = 104 at different distance positioned; (a) L1; (b) L2; and (c) L3*

5. Conclusion

The goal of the present study is to computationally investigate the flow characteristics in the wake of the circular cylinder and plate behind the bluff with varied distanced position ratios under constant Re. This study was made with the help of a finite volume technique using commercial software ANSYS FLUENT at subcritical Reynolds number 104, with distanced ratio as an important factor. The primary findings lead to the following conclusions:

- It is observed that the lift coefficient, C_L, increases along with the distanced position ratio. Anyhow, the L_2 distance provides a better increment.
- Compared to L_2 and L_3, even when the distance increased, the flow carrying high pressure was much higher in L_2. This phenomenon could be reasonable due to the dissemination of the vortex core before reaching the tip of the L_3 plate.
- In turbulence instances, particularly subcritical flow conditions, the amplitude of pressure connected with the wake zone of the cylinder gradually decreases with increasing distance.
- It was observed that with a more significant force coefficient, the lift creates a well for L_2 positions and possibly has better deformation than other positions; this could contribute more development to vibrational-based devices as energy harvesters.

Acknowledgement

This research was made possible by funding from the Fundamental Research Grant Scheme (FRGS/1/2020/TK0/UTHM/02/24) provided by the Ministry of Higher Education (MOHE), Malaysia and supported by Universiti Tun Hussein Onn Malaysia (UTHM) through GPPS (vot H694).

Conflict of Interest

Authors declare that there is no conflict of interests regarding the publication of the paper.

Author Contribution

All authors have contributed to this work.

References

[1] Chakraborty, J., Verma, N., and R. P. Chhabra, Wall effects in flow past a circular cylinder in a plane channel: A numerical study, in *Chemical Engineering and Processing: Process Intensification*,p. 1529-1537, 2004

[2] Meis, M., Varas, F., Velázquez, A., and Vega, J. M., Heat transfer enhancement in micro-channels caused by vortex promoters, in *International Journal of Heat and Mass Transfer*, Elsevier Ltd. p. 29-40, 2010.

[3] Zhang, X., Perot, B., Turbulent vortex shedding from triangle cylinder using the turbulent body force potential model, in *American Society of Mechanical Engineers, Fluids Engineering Division (Publication) FED*, p. 75-80, 2000.

[4] Kulkarni, A.A., Harne, M. S., and Bachal, A., Study of Vortex Shedding Behind Trapezoidal Bluff Body by Flow Visualization Method. p. 1057-1062, 2014.

[5] Sambu, M., Badrin, M. I., Zaman, I., Manshoor, B., Khalid, A., Chan, S. W., and Salleh, M.M., Journal of Complex Flow Flow-Induced Vibration of Cantilever Beam by One-Way Fluid Structure Interaction Approach, in *JCF Journal of Complex Flow*. p. 39-43. 2022.

[6] Shair, F. H., Grove, A. S. , Petersen, E. E., and Acrivos, A., The effect of confining walls on the stability of the steady wake behind a circular cylinder, in *Journal of Fluid Mechanics*. p. 546-550, 1963.

[7] Camarri, S., Salvetti, M. V., and Buresti, G., Large-eddy simulation of the flow around a triangular prism with moderate aspect ratio, in *Journal of Wind Engineering and Industrial Aerodynamics*. p. 309-322, 2006.

[8] Singh, J., Agrawal, T., and Yadav, S., Study of vertex shedding phenomenon in the vortex flow meter, in *Materials Today: Proceedings*. 2019, Elsevier Ltd. p. 2977-2983, 2019.

[9] Ricci, M., Patruno, L., Miranda, S. de., and Ubertini, F., Flow field around a 5:1 rectangular cylinder using LES: Influence of inflow turbulence conditions, spanwise domain size and their interaction, in *Computers and Fluids*. Elsevier Ltd. p. 181-193, 2017.

[10] Hart, J., Comparison of Turbulence Modeling Approaches to the Simulation of a Dimpled Sphere, in *Procedia Engineering*. p. 68-73, 2016.

[11] Adeyemi, I., Kharoua, N., Khezzar, L., Meribout, M., and AlHammadi, K., Review of confined swirling flows and bluff body impacts on flow and heat transfer characteristics, in *Chemical Engineering Research and Design*. Elsevier. p. 359-386, 2022.

[12] Islam, S. U., Manzoor, R., Islam, Z. U., Kalsoom, S., and Ying, Z. C., A computational study of drag reduction and vortex shedding suppression of flow past a square cylinder in presence of small control cylinders, in *AIP Advances*. 2017.

[13] Kumar, A., and Ray, R. K., Numerical Simulation of Flow Around Square Cylinder with an Inlet Shear in a Closed Channel, in *Lecture Notes in Mechanical Engineering*. p. 297-304, 2018.

[14] Ajoy, D. P., and Das, K.R., A numerical study on effect of corner radius and Reynolds number on fluid flow over a square cylinder, in *Sadhana - Academy Proceedings in Engineering Sciences*. 2017, Springer India. p. 1155-1165.

[15] AkaydIn, H. D., Elvin, N., and Andreopoulos, Y., Wake of a cylinder: A paradigm for energy harvesting with piezoelectric materials, in *Experiments in Fluids*. p. 291-304, 2010.

[16] Ordia, L., Venugopal, A., Agrawal, A.,and Prabhu, S. V., Influence of After Body Shape on the Performance of Blunt Shaped Bodies as Vortex Shedders, in *Internation Journal of Mechanical and Mechatronics Engineering*. p. 836-841, 2013.

[17] Liu, H., Qu, Y., Xie, F., and Meng, G., Vortex-induced vibration of large deformable underwater composite beams based on a nonlinear higher-order shear deformation zig-zag theory, in *Ocean Engineering*. p. 111000, 2022.

[18] Javad Farrokhi Derakhshandeh, Fluid structural interaction of a flexible plate submerged in the wake of a circular cylinder, in *Ocean Engineering*. p. 112933, 2022.

[19] Wang, X., Chen, J., Zhou, B., Li, Y., and Xiang, Q., Experimental investigation of flow past a confined bluff body: Effects of body shape, blockage ratio and Reynolds number, in *Ocean Engineering*. p. 108412, 2021.

[20] Hsu, L. C., and Chen, C. L., The drag and lift characteristics of flow around a circular cylinder with a slit, in *European Journal of Mechanics, B/Fluids*. p. 135-155, 2020.

[21] Okhotnikov, D. I., Molochnikov, V. M., Mazo, A. B., Malyukov, A. V., Goltsman, A. E., and Saushin, I. I., Viscous near-wall flow in a wake of circular cylinder at moderate Reynolds numbers, in *Thermophysics and Aeromechanics*. p. 873-882, 2017.

[22] Sharma, B., and Barman, R. N., Unsteady flow past slotted circular cylinders in laminar regime: Effect of slit shapes and Reynolds number, in *Physics of Fluids*. 2023.
[23] Etminan, A., Bodaghkhani, A., and Muzychka, Y. S., Numerical Simulation of Laminar Vortex-Shedding Flow around a very Slender and Rectangular Bluff Body, in *Journal of Fluid Flow, Heat and Mass Transfer*. p. 37-45, 2020.
[24] Xing, F., and Lei, C., A large eddy simulation of flow over a circular cylinder with circumferential triangular riblets: Effects of spanwise coverage ratio, in *Ocean Engineering*. p. 112439, 2022.
[25] Sun, C., Zhou, T., An, H., Zhu, H., and Cheng, L., On the study of vortex-induced vibration of circular cylinders covered with different roughness, in *Applied Ocean Research*. p. 103215, 2022.
[26] Ferziger, J. H., Perić, M., and Street, R. L., Computational Methods for Fluid Dynamics, Fourth Edition, in *Computational Methods for Fluid Dynamics*. p. 1-596, 2019.
[27] Park, J., and Choi, H., Numerical solutions of flow past a circular cylinder at reynolds numbers up to 160, in *KSME International Journal*. p. 1200-1205 1998.
[28] Chen, W., Ji, C., Alam, M. M., Williams, J., and Xu, D., Numerical simulations of flow past three circular cylinders in equilateral-triangular arrangements, in *Journal of Fluid Mechanics*. p. 1-44, 2020.